

Testing the Trapped Gyro-Landau Fluid Transport Model with Data from Tokamaks and Spherical Tori

G.M. Staebler 1), G. Colyer 2), S. Kaye 3), J.E. Kinsey 1), and R.E. Waltz 1)

1) General Atomics, P.O. Box 85608, San Diego, California 92186-5608, USA

2) EURATOM/UKAEA Fusion Association, Culham Science Centre, UK

3) Princeton Plasma Physics Laboratory, Princeton, New Jersey, USA

e-mail contact of main author: Gary.Staebler@gat.com

Abstract: Results of the first tests of the trapped gyro-Landau fluid (TGLF) transport model with experimental data from the Spherical Tori (ST) MAST and NSTX are reported and compared with recent tests with conventional tokamak data [J.E. Kinsey, et al., Phys. Plasmas **15**, 055908 (2008)] from DIII-D, JET, and TFTR. It is found that TGLF predicts low- k driftwave turbulence is largely suppressed by $E \times B$ velocity shear in the STs resulting in neoclassical ion and high- k electron energy transport being dominant in agreement with previous studies. It is also found that high electron-ion collision rates in the STs eliminate most of the trapped electron drive reducing the energy transport significantly.

The TGLF transport model [1–3] is a reduced theoretical model that has been tested with a large database of nonlinear gyrokinetic turbulence simulations using the GYRO code [4]. The TGLF model accurately computes linear driftwave eigenmodes [1]. The particle and energy fluxes due to these driftwaves are then computed from quasi-linear theory and a simple model for the saturated fluctuation intensity [2,3]. The TGLF model generalizes the methods of its predecessor GLF23 [5] to a more accurate system of moment equations and an eigenmode solution method that is valid for shaped magnetic geometry and finite aspect ratio. Recently, tests of TGLF [3] with a database of 96 discharges (L-mode and H-mode) from three tokamaks were made. It was found that the improved fidelity of TGLF to exact gyrokinetic theory resulted in an improved prediction of the tokamak temperature and density profiles compared to GLF23, strengthening the case for gyrokinetic driftwave turbulence being the dominant energy transport mechanism in tokamaks. As shown in Fig. 1, the plasma-stored energy incremental to the boundary energy was predicted with an RMS error of 19%, and an average offset of 2%. The GLF23 model prediction had an RMS error of 36% and an offset of 16% for this same dataset.

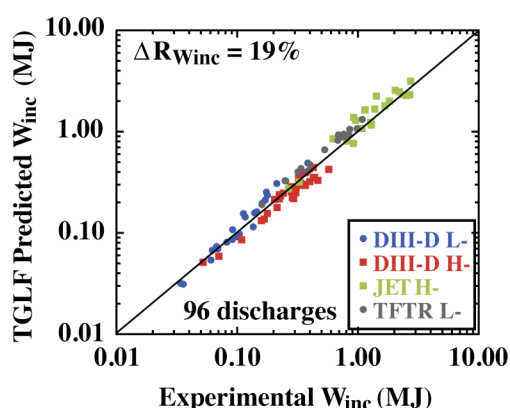


Fig. 1. Incremental stored energy ($W_{inc} = W - W_{boundary}$) predicted by TGLF versus experimental data from 96 tokamak discharges.

For the $s-\alpha$ model geometry [6] (infinite aspect ratio circle) there is an exact scaling from tokamaks to STs. As long as the ratio of the major radius to the temperature and density gradient lengths is held fixed as the major radius is varied, the linear growth rate normalized to the ion thermal velocity divided by the major radius will be invariant (as will the normalized fluxes). If trapped particles are included, then the ratio of the local minor radius

to major radius must be held fixed as well in order to keep the trapped fraction fixed. For the finite aspect ratio Miller geometry model [7], there is no simple scaling with aspect ratio since the aspect ratio directly impacts the curvature drift. Finite aspect ratio is generally destabilizing for the driftwave. This effect is validated by the better prediction of TFTR circular discharges with the Miller model geometry than with $s - \alpha$ for TGLF [3].

The Miller model also includes elongation and triangularity in an up-down symmetric flux surface shape. The shape parameters input into the model are obtained from a numerical solution of the Grad-Shafranov equilibrium equation. The Miller model is only close to the equilibrium solution if the actual shape of the flux surfaces are well fit by the Miller model. TGLF is the first theory based transport model that is not limited to large aspect ratio circular flux surfaces ($s - \alpha$ model).

Controlled experiments varying the elongation of flux surfaces on the DIII-D tokamak have observed an improvement of energy confinement with increasing elongation [8]. This trend is also seen in flux tube nonlinear GYRO simulations [9]. As shown in Fig. 2, the TGLF model matches the GYRO simulations well as elongation (and elongation shear) is varied about a standard reference case. The electron and ion temperature profiles predicted by TGLF are found to be a good match to the DIII-D elongation experiments, indicating that the impact of elongation on driftwave-induced transport accounts for the change in energy confinement observed in the experiment.

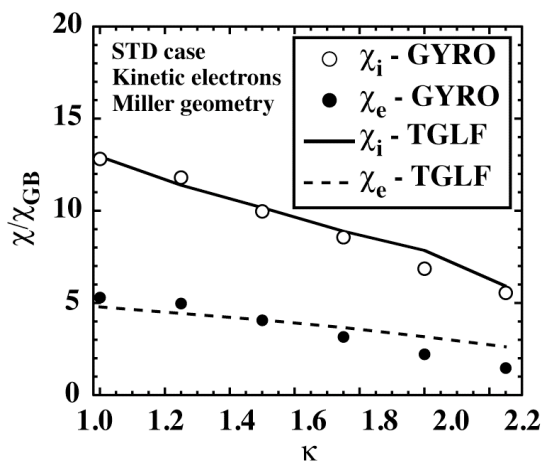


Fig 2. Elongation scan about a standard reference point comparing the TGLF quasi-linear transport model with nonlinear GYRO simulations.

High wave number electron temperature gradient (ETG) modes are predicted to play a dominant role in electron energy transport in NSTX [10]. Trapped electron physics and ETG mode transport are more accurately modeled in TGLF than in GLF23. The trapped particle model in TGLF enables the same system of moment equations to be valid for both trapped and passing particles continuously from low to high poloidal wavenumber. Transport due to driftwaves is strongly peaked at low wavenumber. However, equilibrium $E \times B$ velocity shear preferentially suppresses low wave-number turbulence due to the low growth rates of these modes [11]. Thus, as $E \times B$ velocity shear increases, so does the importance of the higher wavenumber modes. Defining the effective electron thermal diffusivity of the high- k modes as the total effective electron thermal diffusivity (including neoclassical) minus the contribution from the TGLF model for modes with poloidal wavenumbers times the ion gyroradius less than one, the relative contribution from the high- k modes can be monitored. The typical L-mode DIII-D discharge in Fig. 3(a) has a low $E \times B$ velocity shear and a low fraction of the electron energy flux produced by the high- k modes. The H-mode in Fig. 3(b) has a higher fraction of high- k electron energy transport because the higher toroidal rotation of the H-mode suppresses the low- k modes. The hybrid discharge in Fig. 3(c) has an even higher $E \times B$ velocity shear suppressing most of the low- k modes so that almost all of the electron energy transport is from high- k modes. Note that the ion transport is reduced to near neoclassical when the low- k modes are suppressed.

The low-field ST's NSTX and MAST differ from the tokamaks in the database of Fig. 1 in one other important respect. The electron-ion collision frequency is an order of magnitude larger. This has a strong stabilizing influence on the driftwaves since it eliminates most of the trapped electron drive. Comparing the collision model used in the tokamak test (APS07 version) [3] with the exact gyro-kinetic turbulence code GYRO at the much higher collision frequencies of the STs, it was found that the APS07 version predicted ion energy fluxes that were significantly too high. The APS07 collision model for TGLF was fit to a set of linear growth rates from exact gyro-kinetic calculations. The closure for TGLF, and all other gyro-fluid models, was fit to the moments of a local collisionless gyro-kinetic solution for the perturbed distribution function. Since Ref. [3] was published, a major upgrade of the electron-ion collision model has been developed. The new model is fit to a local numerical solution to the gyro-kinetic equation with pitch-angle scattering of electrons. The details of this model will be published elsewhere. The new collision model is fit to the local kinetic response function not to individual linear or non-linear gyro-kinetic results. Hence, it should be valid for the full range of plasma parameters and geometry for which the gyro-kinetic equation is valid. However, the transport fluxes have only been compared to two collision scans using GYRO and a handful of gyro-kinetic linear stability results to date. Thus, the results of this paper are preliminary and the collision model may need to be changed in the future if serious differences with GYRO are discovered.

The first tests of TGLF with ST data will now be presented. A set of 8 MAST and 5 NSTX discharges were selected and run through the TRANSP analysis code [12] to compute the fast ion density and heating sources. Only single time slice TGLF steady state runs were used (like the tokamak tests). The ST discharges were not stationary. In order to minimize the time derivative corrections to the energy and particle sources, times near the peak in the total stored energy were selected. The TGLF code only computes transport fluxes due to driftwaves when run electrostatically as was done for this study. The neoclassical fluxes are added to this. If there are MHD modes like sawteeth or tearing modes they can also produce transport. The transport code (XPTOR) used to run TGLF enhances the electron neoclassical thermal diffusivity to the ion neoclassical level when the safety factor (q) is less than one to crudely estimate the sawtooth induced transport. Since TGLF is not determining the transport in this region, it will be excluded from our calculation of the deviation between TGLF temperature predictions and the data. Only one of the 8 MAST discharges had $q > 1$ everywhere at the time of peak stored energy so it is the best case to test TGLF. This

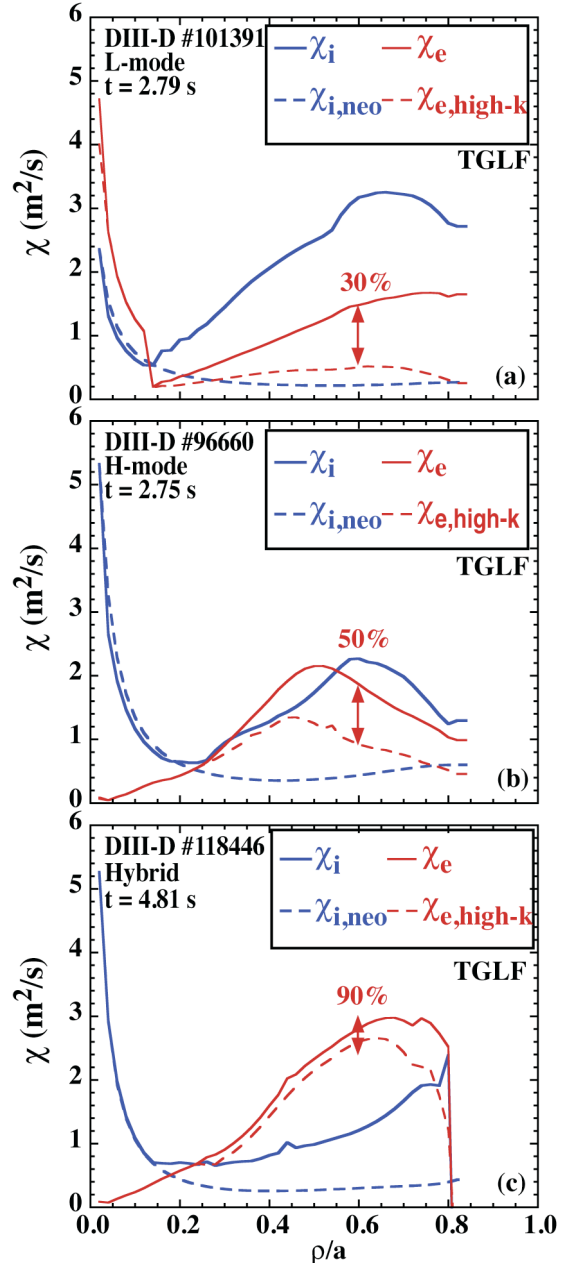


Fig. 3. Effective energy diffusivities predicted by TGLF for an L-mode (a) and H-mode (b) and a hybrid mode (c) discharges in the DIII-D tokamak.

discharge (8500) has been the subject of linear gyrokinetic stability study [13]. It is an H-mode discharge. The safety factor, elongation and average triangularity of the flux surfaces for 8500 at 0.2745 s are shown in Fig. 4. The q -profile has a weakly negative magnetic shear near the axis but $q > 1$ everywhere for this discharge. The TGLF predicted electron and ion temperature profiles are compared with curves fit to the MAST data in Fig. 5. The new TGLF collision model is used. The toroidal rotation and density profiles were not evolved by TGLF but were taken from the data. The boundary of the simulation was taken at $\rho/a = 0.82$. The

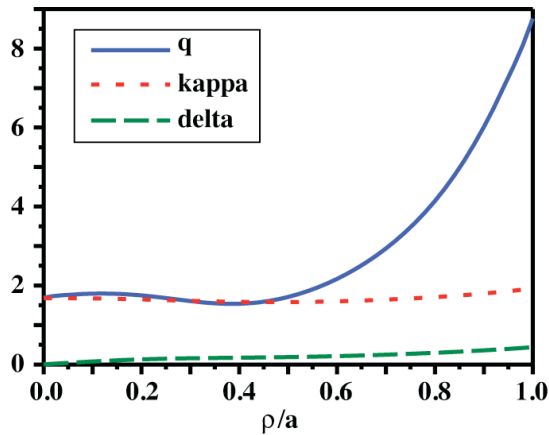


Fig. 4. Profile of the safety factor, elongation and triangularity for MAST discharge 8500@ 0.2745 s.

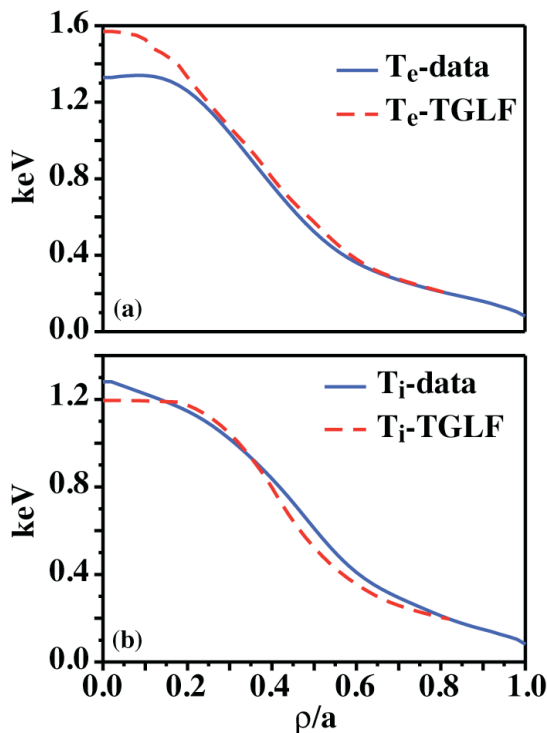


Fig. 5. Electron (a) and ion (b) temperature profiles predicted by TGLF (dashed) compared with a curve fit to measured data (solid) for MAST discharge 8500@ 0.2745 s.

effective energy diffusivities [$\chi = -Q/(ndT/dr)$] from TGLF are shown in Fig. 6. The ion energy diffusivity is reduced to the Chang-Hinton neoclassical level (χ_i^{C-H}) inside of $\rho/a = 0.5$. In this same region, the high- k electron energy transport (χ_e^{high-k}) becomes dominant. The high- k modes produce a small ion energy pinch at about $\rho/a = 0.35$. Remarkably, the electron energy diffusivity is reduced to electron neoclassical in the deep core $\rho/a < 0.15$. The XPTOR code approximates the electron neoclassical diffusivity by multiplying the ion thermal diffusivity by the square root of the electron to ion mass ratio. The transport in this MAST discharge is similar to the hybrid tokamak discharge in Fig. 3(c). The ion energy transport is nearly neoclassical over a large region and the electron energy transport is dominated by the high- k modes. The low ion transport is caused by the $E \times B$ velocity shear suppression of the low- k modes in both the MAST H-mode and DIII-D hybrid discharges. Turning off the $E \times B$ velocity shear “quench rule” [11] in TGLF results in much colder predicted temperatures. These transport results are in agreement with previous analysis of MAST [13] and NSTX discharges [10].

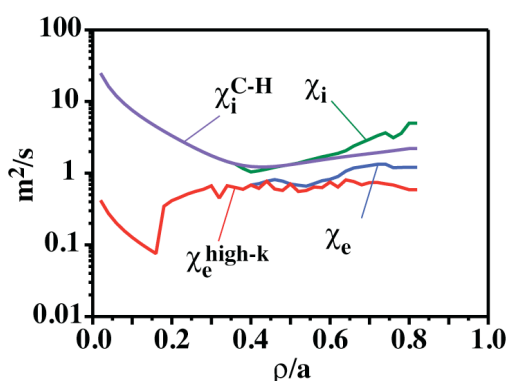


Fig. 6. Effective energy diffusivities for MAST discharge 8500 @0.2745 s.

The good results for this discharge were obtained with a modified neoclassical model in XPTOR. The recently developed NEO code [14] provides a high accuracy numerical calculation of neoclassical transport. Comparison of the NEO results with analytic formulas has shown that the Chang-Hinton formula for ion thermal diffusion should be modified to use an effective magnetic field (B_unit) in the calculation $B_unit = B_0 \rho / r d\rho / dr$, where B_0 is the vacuum magnetic field at the magnetic axis, r is the minor radius of the flux surface and ρ is defined so that the toroidal flux = $\pi \rho^2 B_0$. Even with this modification, the Chang-Hinton formula tends to be larger than the NEO calculation. Including various published impurity corrections to Chang-Hinton only makes the gap with NEO larger [14]. Hence, we used the Chang-Hinton formula with B_unit and a pure plasma formula. The impact of using B_0 instead of B_unit is illustrated in Fig. 7. The predicted electron temperature profile in Fig. 7(a) using B_0 (green dotted) is little changed from the reference with B_unit (blue solid) but the ion temperature is reduced significantly in Fig. 7(b). The only change here was in the neoclassical model. Due to the strong impact of neoclassical transport on the MAST temperature predictions, it would be worthwhile to replace the Chang-Hinton formula with the NEO calculation in the transport code in the future. The electron-ion collision model also has a significant impact. In Fig. 7 (red dashed curves) are shown the predicted temperatures using the APS07 version [3] of the TGLF collision model (but using B_unit in Chang-Hinton). The stronger low- k transport of this model results in reduced ion and electron temperatures. Recall that at the high collision frequency of MAST, the ASP07 collision model predicts too large an ion energy transport compared to non-linear GYRO simulations. The APS07 model is close to the new collision model for the low collision frequency typical of the tokamak data test of Ref. [3]. The new model has not yet been tested on the tokamak database but it's improved fidelity to GYRO for high collision frequency does produce a better agreement with this MAST data.

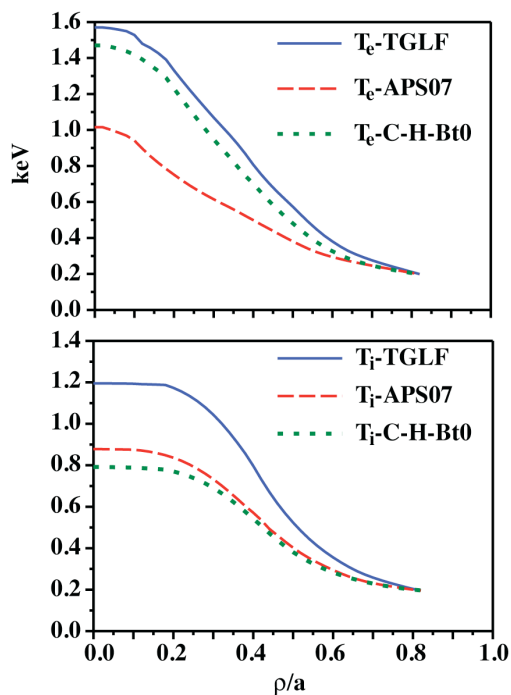


Fig. 7. The variations of the electron (a) and ion (b) temperature profiles predicted by XPTOR for MAST discharge 8500. (solid blue) TGLF with the new collision model and using B_{unit} in the Chang-Hinton neoclassical formula (C-H). (red dashed) TGLF with the APS07 version of the collision model (dashed) or and B_{unit} in C-H. (green dotted) TGLF with the new collision model but using the vacuum magnetic field B_0 in the Chang-Hinton neoclassical formula.

Turning on the TGLF electron density evolution gives the density profile prediction in Fig. 8. The hollow density profile is transient and the particle flux is negative in the core due to the time derivative corrections to the particle source.

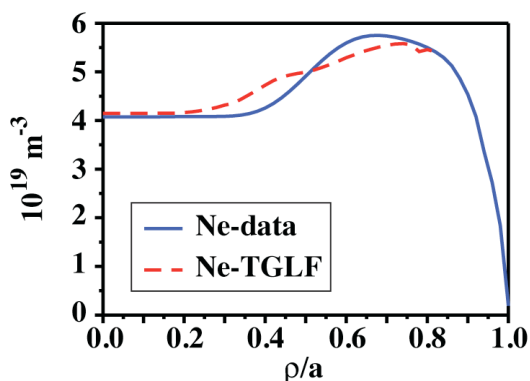


Fig. 8. Electron density profile predicted by TGLF compared to a curve fit to measured data for MAST discharge 8500@0.2745s.

Surprisingly, the impact of Miller geometry on this MAST discharge was not strong. Using the $s-\alpha$ model lowers the temperatures a little. This discharge has enough shaping to reduce the transport and compensate for the increase due to finite aspect ratio for Miller geometry giving little net change compared to the $s-\alpha$ model. This cancellation between the impacts of shaping and aspect ratio in Miller geometry was also found to be the case for the shaped tokamaks DIII-D and JET but not for the circular tokamak TFTR [3]. Modeling circular MAST discharges would better test the impact of finite aspect ratio.

The remaining 7 MAST discharges all had a $q=1$ surface at about $\rho/a = 0.4-0.5$. Inside of this radius the predicted temperature profile was typically too hot for the electrons indicating that the electron thermal transport was much larger than the ad-hoc ion neoclassical level imposed by XPTOR. It can be concluded from this that the driftwave transport is not the dominant transport mechanism in the MHD unstable region $q < 1$. The statistics for the predicted ion and electron temperature profiles outside of the $q=1$ surface for the MAST discharges at the peak of the stored energy are given in Table 1. The

definitions of the fractional deviation σ_{T_s} and offset f_s^{offset} for species ($s = e, i$) outside the $q = 1$ surface are:

$$\sigma_{T_s} = \frac{1}{T_s^{norm}} \sqrt{\int_{\rho_{q=1}}^{\rho_{boundary}} \frac{d\rho}{\Delta\rho} (T_s^{TGLF} - T_s^{data})^2},$$

$$f_s^{offset} = \frac{1}{T_s^{norm}} \int_{\rho_{q=1}}^{\rho_{boundary}} \frac{d\rho}{\Delta\rho} (T_s^{TGLF} - T_s^{data}),$$

$$T_s^{norm} = \sqrt{\int_{\rho_{q=1}}^{\rho_{boundary}} \frac{d\rho}{\Delta\rho} (T_s^{data})^2}, \quad \Delta\rho = \rho_{boundary} - \rho_{q=1}.$$

TABLE 1: STATISTICS FOR MAST DISCHARGES.

MAST Discharge No.		Deviation- T_i	Deviation- T_e	Offset- T_i	Offset- T_e
8500	H-mode	0.057	0.104	-0.035	0.070
18571	H-mode	0.225	0.243	-0.125	-0.138
15021	H-mode	0.098	0.639	-0.056	0.353
8505	L-mode	0.219	0.050	-0.127	0.010
17661	L-mode	0.147	0.127	-0.003	0.003
17663	L-mode	0.291	0.267	0.050	0.042
17666	L-mode	0.133	0.307	0.053	0.186
17668	L-mode	0.171	0.300	-0.022	0.133
Average		0.167	0.255	-0.033	0.082

The ion offsets are mostly negative indicating the predicted ion temperature is on average less than the data. Most of the electron offsets are positive so TGLF is systematically too hot. The average fractional deviations are 16.7% for the ion temperature and 25.5% for the electron temperature. These are comparable to the results for the Tokamak database [3] (T_i -15%, T_e -16%) which is promising but the sample size here is very small. These are the statistics from the $q=1$ surface (typically $\rho/a = 0.45$ for all but 8500) to the boundary at $\rho/a = 0.82$ which is a smaller fraction of the profile than for the typical Tokamak cases in Ref. [3].

The five NSTX discharges that were modeled ran into problems with convergence of the Newton-implicit solver in the XPTOR code. One difference between NSTX and MAST for these discharges is that for NSTX $q > 1$ everywhere even at the time of peak stored energy. This does not necessarily mean that the discharges were stable to resistive interchange modes. It has been observed [15] in linear stability analysis of negative central shear discharges on DIII-D that even though $q > 1$ the negative magnetic shear region can be resistive interchange unstable with a dramatic impact on the electron thermal transport. In the region where the resistive interchange mode is computed to be unstable, the electron temperature profile was found to be very flat. However, linear gyrokinetic stability calculations found that the electron temperature gradient threshold for high- k ETG modes was very high in this region. For the NSTX discharges the ETG threshold electron temperature gradient computed using TGLF becomes larger than the measured gradient for $\rho/a < 0.4$. Clearly a better understanding of the relationship between large scale MHD and small scale driftwave stability and transport is needed. The MAST discharges had similar convergence problems for TGLF when $q < 1$. For most cases, the transport code only converged if TGLF was turned off when $q < 1$ leaving the neoclassical ion energy and ad-hoc electron energy transport in this region. For the MAST cases where TGLF converged for $q < 1$, the electron temperature prediction was far above the data in this region indicating that the ETG modes were not the dominant transport mechanism there. Computing the energy

fluxes with TGLF using the measured NSTX temperature profiles gives qualitatively similar results as for MAST, in that low- k modes are suppressed by $E \times B$ shear over most of the core and high- k modes provide the remaining electron energy flux. All of the drifwaves are stable in the deep core ($\rho/a < 0.4$) for the NSTX data indicating that there is some other transport mechanism at work here. Including full electromagnetic fluctuations (both parallel and perpendicular magnetic flutter) in TGLF only stabilized the low- k drifwaves further. No kinetic ballooning modes were unstable in the five discharges considered.

This first test of TGLF with data from the spherical tori MAST and NSTX has found that the ion thermal transport is dominated by neoclassical over much of the plasma. The ion temperature gradient mode is only active in the outer quarter and is suppressed by $E \times B$ velocity shear elsewhere. The Chang-Hinton formula, modified by using B_{unit} as proposed in Ref. [11], provides about the right level of ion thermal transport since the ion temperature is well predicted with a small negative offset. In the region outside the $q = 1$ surface the electron thermal transport is predominantly high- k ETG modes with low- k modes doubling the diffusivity in the outer quarter of the profile. The trapped electron modes are suppressed by the high frequency of electron-ion collisions. The predicted ion and electron temperatures in this region are in good agreement with the MAST data. The electron thermal transport computed by TGLF is somewhat low since the predicted electron temperature is systematically high. This could be due to the new collision model in TGLF giving too much trapped electron suppression or the saturation rule giving too small a contribution from the high- k modes. This result identifies the need for non-linear gyrokinetic simulations of STs including electron-ion collisions and ETG modes in order to refine the TGLF saturation rule for high- k modes, which is based on a single collisionless GYRO run. In the MHD unstable region ($q < 1$), the high- k driftwave transport in TGLF was far too weak indicating a much stronger electron energy transport mechanism is at work. Even though $q > 1$ in the NSTX discharges studied, the threshold electron temperature gradient of ETG modes computed using TGLF is well above the experimental value for $\rho/a < 0.4$ suggesting MHD activity in this region. Kinetic ballooning MHD modes were computed to be stable using TGLF however.

Acknowledgment

This work was supported in part by the US Department of Energy under DE-FG02-95ER54309 and DE-AC02-76CH03073, by the UK Engineering and Physical Sciences Research Council and by EURATOM.

References

- [1] STAEBLER, G.M., KINSEY, J.E., and WALTZ, R.E., Phys. Plasmas **12**, 102508 (2005).
- [2] STAEBLER, G.M., KINSEY, J.E., and WALTZ, R.E., Phys. Plasmas **14**, 055909 (2007).
- [3] KINSEY, J.E., STAEBLER, G.M., and WALTZ, R.E., Phys. Plasmas **15**, 055908 (2008).
- [4] CANDY, J., and WALTZ, R.E., J. Comput. Phys. **186**, 545 (1003).
- [5] WALTZ, R.E., STAEBLER, G.M., DORLAND, W., HAMMETT, G.W., KOTSCHENROUTHER, M., and KONIGS, J.A., Phys. Plasmas **4**, 2482 (1997).
- [6] CONNOR, J.W., HASTIE, R.J., and TAYLOR, J.B., Phys. Rev. Lett. **40**, 396 (1978).
- [7] MILLER, R.L., CHU, M.S., GREENE, J.M., LIN-LIU, Y.R., and WALTZ, R.E., Phys. Plasmas **5**, 973 (1998).
- [8] LUCE, T.C., PETTY, C.C., and KINSEY, J.E., Proc. 28th EPS Conf. on Control. Fusion and Plasma Phys., Funchal, 2001, ECA Vol. 25A (2001) 1377-1380.
- [9] KINSEY, J.E., WALTZ, R.E., and CANDY, J., Phys. Plasmas **14**, 102306 (2007).
- [10] KAYE, S.M., et al., Nucl. Fusion **47**, 499 (2007).
- [11] WALTZ, R.E., KERBEL, G.D., HILOVICH, J., and HAMMETT, G.W., Phys. Plasmas **2**, 2408 (1995).
- [12] TRANSP is a transport analysis code. For up to date information go to <http://w3.pppl.gov/transp/>
- [13] ROACH, C.M., et al., Plasma Phys. Control. Fusion **47**, B323 (2005).
- [14] BELLI, E., and CANDY, J., Plasma Phys. and Contr. Fusion **50**, 095010 (2008).
- [15] STALLARD, B.W., et al., Phys. Plasmas **6**, 1978 (1999).